NUCLEAR EFFECTS IN LEADING PARTICLE PRODUCTION BY 800-GEV PROTONS

Carol Johnstone
for the E706 Collaboration
Fermilab, Michigan State, Northeastern, Oklahoma,
Penn State, Pittsburgh, Rochester, U.C. Davis

Abstract

Leading particle production by 800-GeV incident protons has been measured at a secondary energy of 530 GeV on seven nuclear targets ranging from beryllium to lead. The nuclear dependence of particle production, in particular, the meson to baryon production ratio is presented here. A new concept in differential Cherenkov counters which uses quartz, plano-convex spherical lenses and high-reflectance, laser dielectric mirrors for light collection and separation allowed data to be taken simultaneously on the three significant leading particles species, pions, kaons, and protons/antiprotons. A separation of pions from kaons was achieved at this energy.

Introduction

Leading particle production by 800-GeV protons on various nuclei was measured in the MWEST secondary beamline at Fermi National Accelerator Laboratory. The production measurements were made at a secondary beam energy of 530 GeV on seven nuclear targets which ranged in weight from beryllium to lead. The data were taken using a helium-filled differential Cherenkov counter enhanced with laser optics to optimize light collection and multiple detection channels. The detection channels were capable of resolving and identifying the different particle types composing the secondary beam. At a specific pressure, data were obtained on the three major leading particle species, pions, kaons, and protons, simultaneously. Because of this feature production measurements were accomplished in about an hour. Detailed pressure curves across all channels were also obtained for the highest and lowest atomic weight targets (lead and beryllium). From the pressure curves, peak shapes and absolute normalizations were ascertained for the separate detection channels.

The Experiment

The experiment was performed in the MWEST beamline which consisted of a 800-GeV primary proton line and production target followed by a secondary beamline. The secondary beamline was capable of selecting and transporting a beam with an energy in the range 25-800 GeV and a momentum bite of +/−6% (RMS, half width). For a positive 530-GeV secondary beam, the target was positioned to create a 1.4 mr production angle with

respect to the secondary beamline. A series of dipoles performed the momentum selection followed by a long parallel section in the beam optics to accomodate the Cherenkov counter. The effective beam divergence at the experiment was +/−.10 mr in the horizontal and +/− .15 mr in the vertical.

The production targets were mounted on a wheel containing 8 slots, seven of which were occupied by the targets, beryllium, carbon, aluminum, copper, tin, tungsten, and lead. In the order given, the targets were .111, .140, .111, .1, .107, .112, and .111 interaction lengths. The eighth slot was left vacant for background measurements.

For part of the run the production target was replaced by pinhole collimators to transport 800-GeV protons to the experiment. Therefore, 800-GeV proton data were obtained in addition to the 530-GeV data. The narrow, pinhole-collimated, 800-GeV proton beam served to calibrate the various channels of the counter and obtain their actual efficiencies. The response of the counter to the much larger, more divergent 530-GeV beam was quantified by comparing 530-GeV pressure curve data with the 800-GeV data.

Technical Description of the MWEST Cerenkov Counter

As previously stated, the Cherenkov was a modified differential one. Its overall length, and, correspondingly, the length of the radiator (which was helium) totaled 138'. At the exit of the counter, an 18"-diameter, aluminized spherical mirror with a focal length of 106' collected and focussed Cherenkov light from different particle types into annular rings. (The upstream section of the counter extended past the light collection optics by 32' to increase the length of the radiating medium.) The light collection optics positioned at the focal plane of the mirror consisted of four sets of laser-grade, quartz lenses (six per set), a pair of aluminized cylinders, optical mirrors and filters, and three rings of high-gain, single photoelectron photomultipliers (Figure 1).

Each of the three rings of photomultipliers tagged one of the three particle types (Figure 2). At the standard operating pressure, the outermost ring of phototubes was illuminated by π light so it was designated the π channel and used to tag pions (Figures 1 and 2). Correspondingly, the middle ring of phototubes was christened the p channel and the inner ring the K channel. The inner ring of phototubes was illuminated through mirrors which will be described later in the section. Because of the large spacing of the outermost set of lenses with respect to the next ring of lenses (for mounting purposes), two reflective, tapered cylinders had to encircle the outer lens ring in order to direct light up and into that channel (see Figure 1).

The proximity of the π and K light and their chromatic overlap at 530 GeV increased the complexity of the optics required to tag Ks and minimize leakage of kaon light into the π channel. To this end the three outer sets of lenses focussed onto the outer ring of phototubes, but their focii were spaced .5" apart so that filtering optics could be installed between the individual lenses and tubes (Figure 1). This allowed 300-600 nm K light from the third ring of lenses to be intercepted by aluminum mirrors which then directed the kaon light through another set of mirrors into the inner ring of photomultipliers. Light passing through the second ring of lenses was also intercepted by mirrors, high-reflectance, 248 nm excimer ones, which reflected ultraviolet light from kaons in the range 200–300 nm, but transmitted the overlapping 300-600 nm pion light (Figure 1). The net effect was to

filter and redirect kaon light into the inner ring of phototubes, or K channel, at the same time allowing pion light to pass into the outer channel of tubes. Light striking outside the second ring of lenses hit the aluminized cylinders first, which had the effect of absorbing the far ultraviolet kaon light (less than 200 nm) and reflecting the pion light (200-300 nm) into the first or outermost set of lenses. These lenses in turn focussed directly onto the outer ring of tubes or π channel. The end result was to reflect the majority of the kaon light into the inner ring of photototubes, providing a K tag and filtering kaons out of the π signal.

For the production data, the counter was operated at 6.2 psi and 17^0 C for 530 GeV beam. This corresponded to an He density of 10^{22} $atoms/cm^2$. At this operating point, the radii of the Cerenkov light at the focal plane of the mirror were 6.74", 6.66" and 6.37" for pions, kaons, and protons, respectively at 300 nm. This meant that Cherenkov light from the three particle types fell into their respective detection channels.

The Data

Pressure curves starting about 5 psi (of He) and ending at 8 were taken using pinhole collimated 800-GeV protons from the primary line. Figure 3 shows an example of the 800-GeV proton data which were valuable for calibrating the actual efficiencies of the p, π, and K channels. In Figure 3 the three- plus higher-fold coincidence rates were normalized to the beam counts and then plotted as a function of pressure for the three channels. The measured single-tube efficiencies of the three channels were 50%, 40%, and 40% for the p, K, and π channels, respectively for 800-GeV beam. For two-fold or more tube coincidence data, the resulting tagging efficiencies of the three channels were then 97%, 80% , and 80%, again for the p, K, and π channels, respectively. Because of preamplification which allowed the tubes to be run at 1800 V or less, the counter was able to trigger at rates that measured up to 10 MHz without evidence of sagging in the bases. (The experiment typically took beam from 1-8 MHz during the Tevatron spill which occurred for approximately 20 sec every minute.)

Two pressure curves were taken, one on the lowest and one on the highest atomic weight targets, to check the systematics in the performance of the counter and obtain absolute normalizations for the beam content. The 5-fold tube coincidence rates from the pressure curves on beryllium and lead are shown in Figure 4. No fundamental differences were observed between the two data sets (other than differences in the leading particle composition). The expanded beam size, momentum spread, and divergence reduced the overall tagging efficiencies and resolution of the counter for 530-GeV beam. The net single-tube firing efficiencies measured for both the beryllium and lead data were 60%, 34%, and 30% for the p, K, and π channels, respectively.

The composition of the secondary beam was calculated by exploiting the specific relationship between the different N-fold coincidence levels. First, the K to π beam content ratio was determined directly from the relatively uncontaminated K and π peaks measured in the 5-fold and 6-fold tube coincidence data taken in the K channel pressure curve data (Figure 4). (Only pressure curve data for the small differential K ring were used to determine the absolute beam composition.) The K/π ratio obtained in this fashion for Be

was .18. The 3-fold and 4-fold coincidence K data were then corrected for π contamination to reproduce this ratio. To effectively eliminate beam composition fractions from the data, ratios were taken between the 3, 4, 5, and 6-fold K and π data separately. Tube firing efficiencies were fit to these K and π ratios. (The ratios between the various N-fold coincidence levels uniquely reflect the actual tube firing efficiencies.) Consistent tube firing efficiencies were found independently for the K and π data (as measured in the K channel). Once the individual tube firing efficiencies were determined for the K channel of tubes, 3 to 6-fold probabilities could be computed. The scaling factor then required to equate the N-fold firing probabilities with the actual values measured for the different N-fold coincidence levels was in fact the fraction of that type of particle in the beam. Because of the high beam rate, the same procedure could not be applied to the proton data. The small 1% probability that two protons traversed the counter simultaneously significantly altered the relationship between consequtive N-fold tube coincidence levels. Instead, the proton fraction was determing using the pion and kaon results.

Beam compositions were calculated for lead and beryllium production targets using the method just stated. Beryllium was found to be 5.36% pions, 1.03% kaons, and 93.61% protons with lead 5.09% pions, 1.20% kaons, and 93.71% protons. Errors will be discussed in the following section. Beryllium was taken as the normalization for the rest of the production data since its pressure curve data were taken subsequent to the particle production data. The lead pressure curve data were taken several hours later than the beryllium pressure curve data.

Production data were measured on all seven targets, including lead and beryllium, by setting the pressure of the counter to center the kaon light in the kaon channel, which then automatically directed the pion and proton light into their respective channels. Several coincidence levels were then measured in the three channels for all targets and subsequently normalized to the beryllium data. Beam composition was then calulated for the other targets relative to beryllium based on the fractions quoted above.

The Results

The beam composition for lead and beryllium (as calculated from pressure curve data) when compared with their respective production data were found to exhibit an overall deviation of 1% in the measured pion content of the beam. This represents an overall systematic error of 17% in the pion fractions presented (the same error assigned to the kaon fractions as well). Given the long-term instability of the secondary line with respect to beam fluctuations, variations in the beam optics (power supply drifts for example), drifts in production angle, etc., this systematic error is not unexpected.

The production data, however, reproduced with a standard deviation of $+/-$ 1% and 4% in the measured pion and kaon fractions, respectively. The increase in the accuracy of the relative measurements is due to the short-term stability in the beam and beamline operation. No statistically significant variation was observed for kaons as a function of atomic weight. Kaons composed aproximately 1.1% of the beam for all targets. (Pion and kaon fractions were corrected for lifetimes.) Pions, however, showed a clear increase in production with increasing atomic weight. Beryllium produced the fewest pions, 5.36%

+/−.05%. That percentage increased steadily as a function of atomic weight until tin, where the pion fraction stablilized at 6.10% +/−.06% of the beam.

References

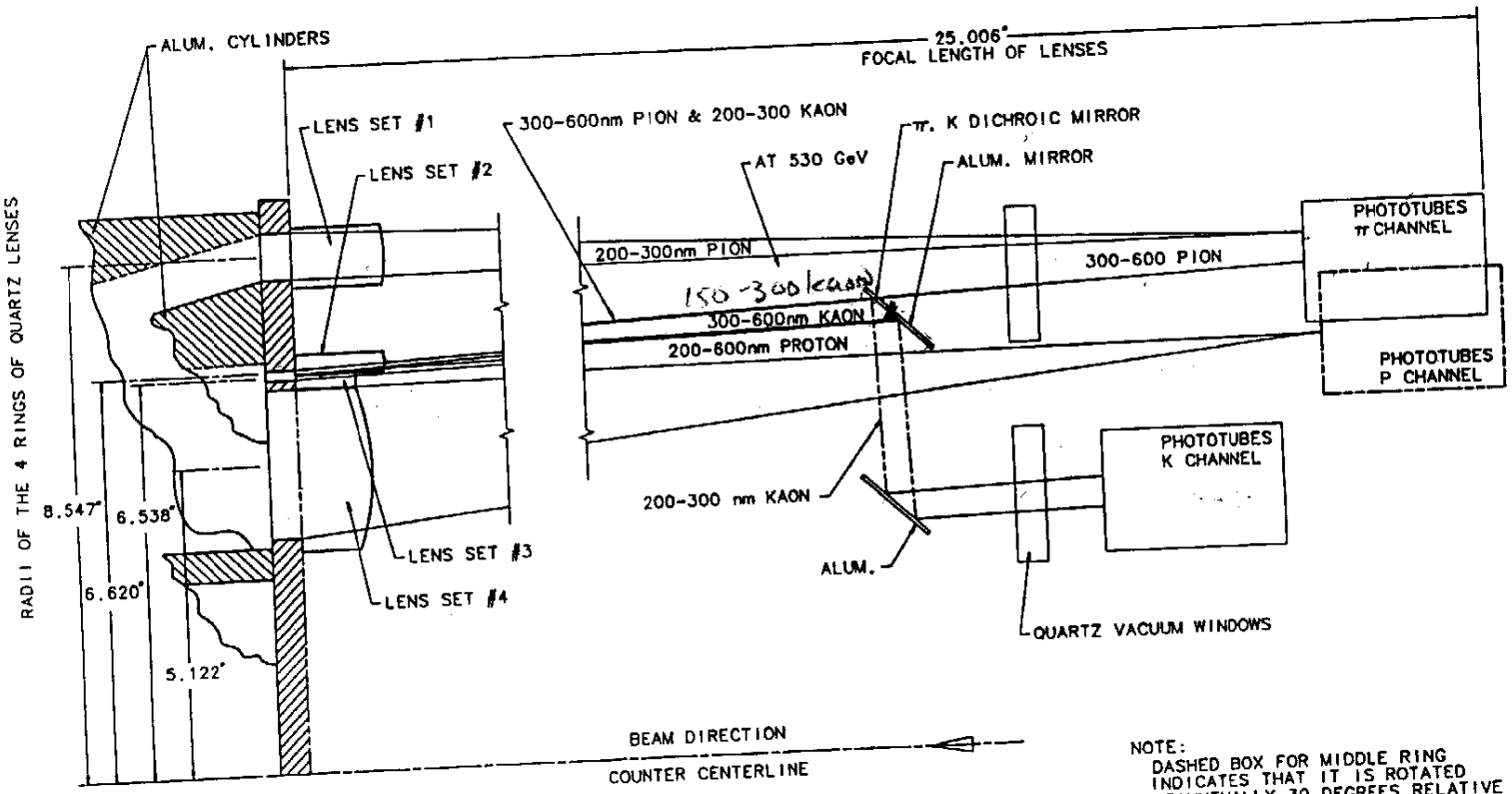

Figure 1. MWEST CERENKOV COUNTER OPTICS

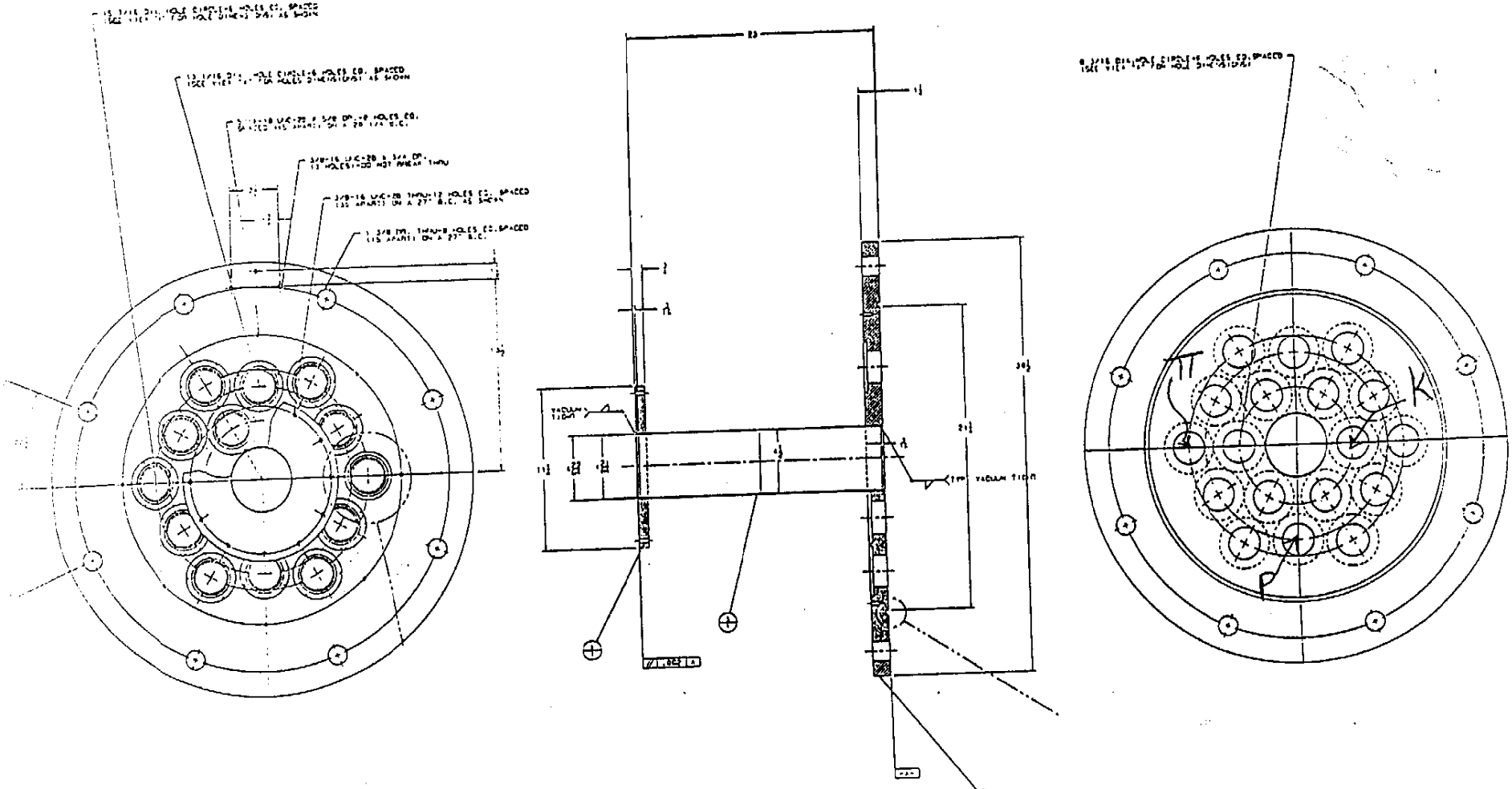

Figure 2. Three rings of photomultiplier tubes--kaon, proton, and pion channels.in order of increasing radius.

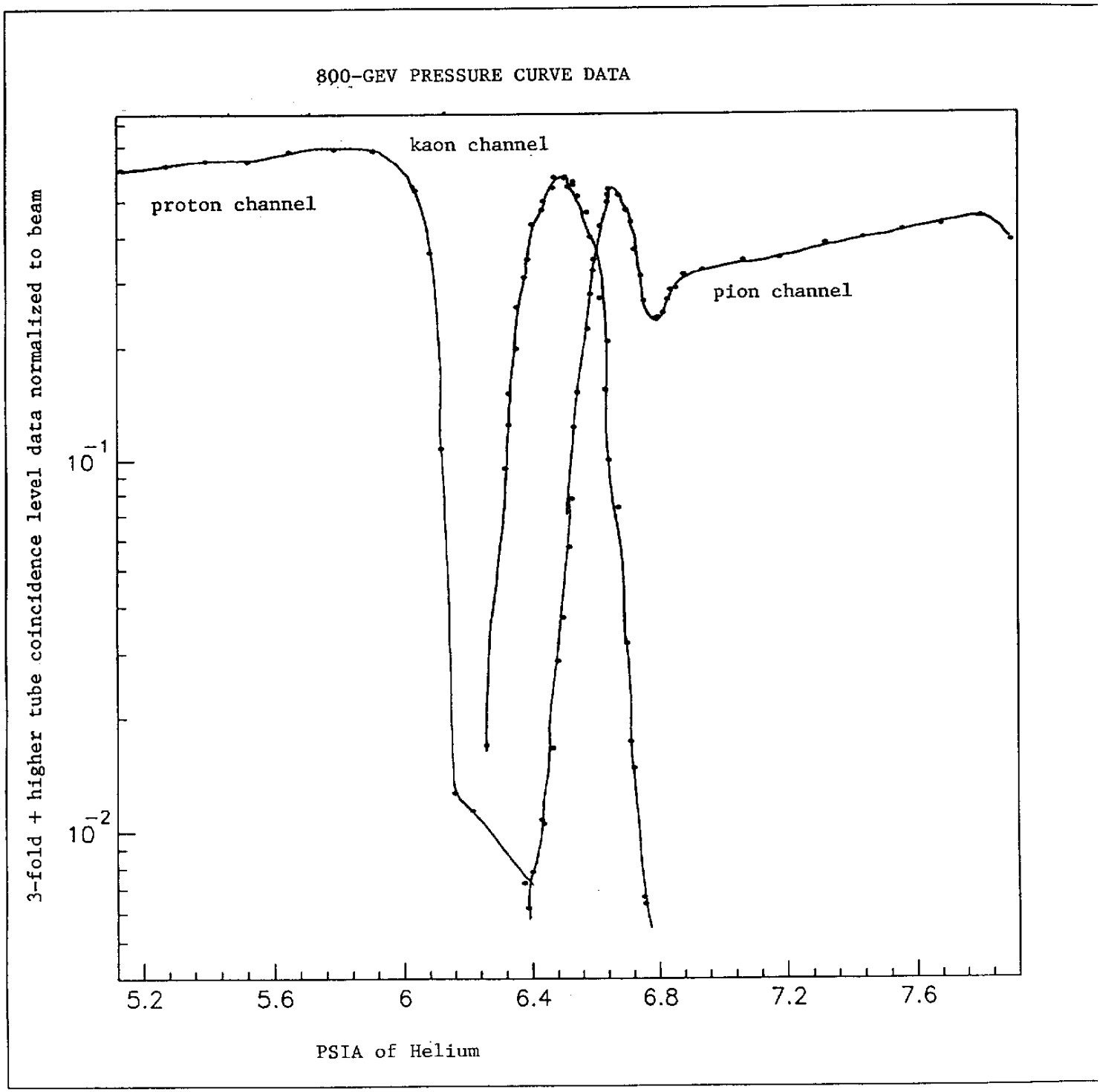

Figure 3. 800-GeV primary proton pressure curve data

The A Dependence of Leading Particle Production by 800 - GeV Protons (530 GeV Secondary Energy)

	$\pi_{fraction}$ %	$K_{fraction}$ %	$P_{fraction}$ %	Secondary Beam Per Primary Proton
Be	5.36	1.03	93.61	$.573 \times 10^{-4}$
C	5.43	1.06	93.51	$.536 \times 10^{-4}$
Al	5.74	1.09	93.17	$.474 \times 10^{-4}$
Cu	5.92	1.10	92.98	$.407 \times 10^{-4}$
Sn	6.13	1.07	92.80	$.325 \times 10^{-4}$
W	6.16	1.08	92.76	$.317 \times 10^{-4}$
Pb	6.15	1.08	92.77	$.329 \times 10^{-4}$
Error	±1%	±4%	±.5%	±.6%

Normalization: extracted from Be pressure curve data

$\pi_{fraction}$	$K_{fraction}$	$P_{fraction}$
5.36 ±.05%	1.03±.05%	93.61±.08%

Table 1. Production Data from target-wheel measurements.

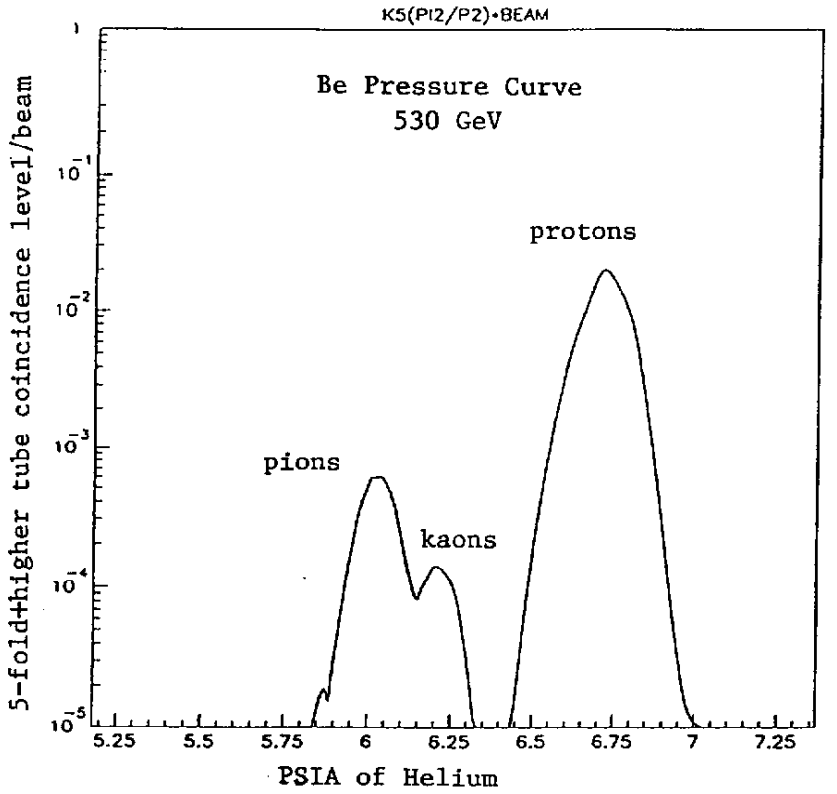

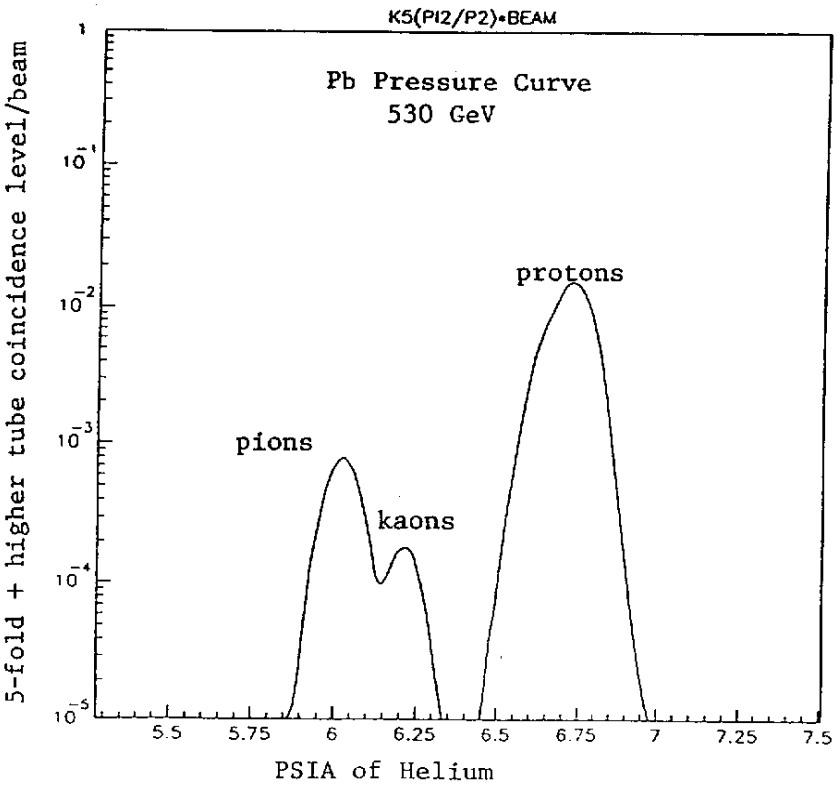

Figure 4. Be and Pb pressure curve data at 530-GeV. Absolute beam composition were determined from these data.

VUV/UV Broadband Coatings

Dielectric Enhanced UV Coatings

The #300-OC coating is a metallic based design with a special dielectric overcoat which offers excellent broadband reflectance from 250nm to 350nm. The #300-OC reflects 95% over this wavelength range, with approximately 70% visible reflectance. If required, the UV reflecting band can be shifted slightly to longer or shorter wavelengths. Angles of incidence other than normal (0°) are available.

Our #250-OC coating was developed to provide enhanced UV reflectance from approximately 235nm to 300nm, with 80-90% visible reflectance.

Dielectric Enhanced UV Coatings

Coating	Reflectance @ N.I.*	Mirror Part # 1.0" dia. x 2.5mm thick
#250-OC	92-95% from 235-300nm	250-OC-FS-1D
#300-OC	95% from 250-350nm	300-OC-FS-1D

*45° reflectance is normally within 2-4% of normal incidence specifications.

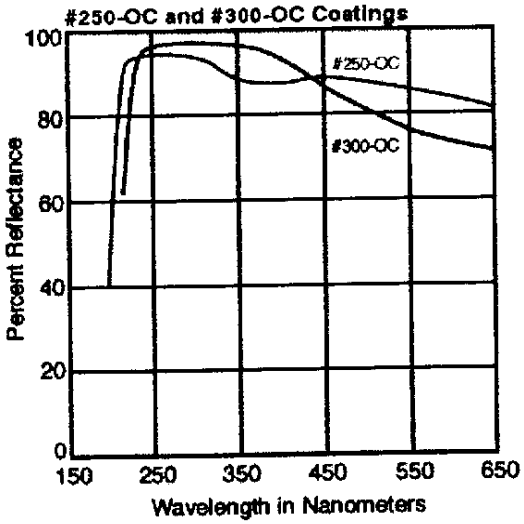

All Dielectric Broadband UV Coatings

Our 308-353-BBFR coating is an all dielectric broadband coating designed to offer maximum reflectance from 308nm to 353nm. Designed primarily as a dual wavelength excimer laser mirror coating, it offers excellent near UV reflectance with an average of 80-90% visible to near IR transmittance.

All Dielectric Broadband UV Coatings

Coating Part #	Reflectance
308-353-BBFR	97 - 99.5%
308-353-BBFR45	95 - 97.5%

Note: Coating shown on graph at right is at 45° AOI.

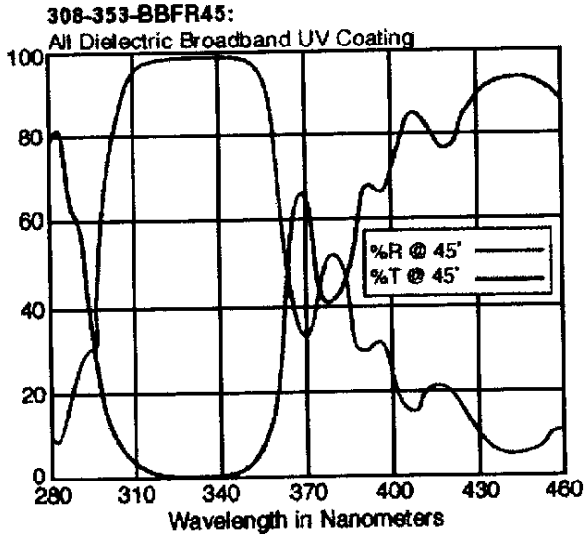

Note: Please contact the Optics Sales Department for information on additional available substrates and their properties. Acton Research routinely coats Customer Supplied Material (CSM). Please call for details.